Electronic Supplementary Material (ESI) for Nanoscale.

Supporting Information

Protic Additives determine the Pathway of CdSe Nanocrystal Growth

Nicholas Kirkwood[a,b] *and Klaus Boldt*[c,*]

[a]School of Chemistry and Bio21 Institute, University of Melbourne, Parkville VIC, 3010, Australia

[b]Current address: Opto-Electronic Materials Section, Faculty of Applied Sciences, Delft University of Technology, Van der Maasweg 9, 2629HZ Delft, The Netherlands.

[c]Department of Chemistry, University of Konstanz, 78457 Konstanz, Germany

Extraction of nanocrystal concentration and diameter from absorbance data.

The concentration of nanocrystals, [NC], can be obtained from size-dependent extinction coefficients:[1]

$$[NC]_{1S} = \frac{A(E)}{\varepsilon(E) l} \cdot \frac{FWHM}{0.12\ eV}$$

Where $\varepsilon(E)$ is the size-dependent per-NC extinction coefficient, $A(E)$ the 1S absorbance, l the path length, and FWHM the 1S absorbance peak full-width half maximum (in eV). Alternatively [NC] can be calculated from the size-independent absorbance coefficient at 3.76 eV, α(3.76 eV) = 1.5 × 10^5 cm^2:

$$[NC]_{3.76\ eV} = \frac{1000 \ln(10) \cdot A(3.76\ eV)}{N_A \cdot V_{QD} \cdot \alpha(3.76\ eV)}$$

Where A(3.76 eV) is the absorbance of the NC ensemble at 3.76 eV (330 nm). However, due to the convolution of absorbance from intermediates such as CP-350 and MSC-437 with the regular NC absorbance spectrum at 3.76 eV, $[NC]_{3.76\ eV}$ over-estimates the true NC concentration in our reactions (see Figure S1).

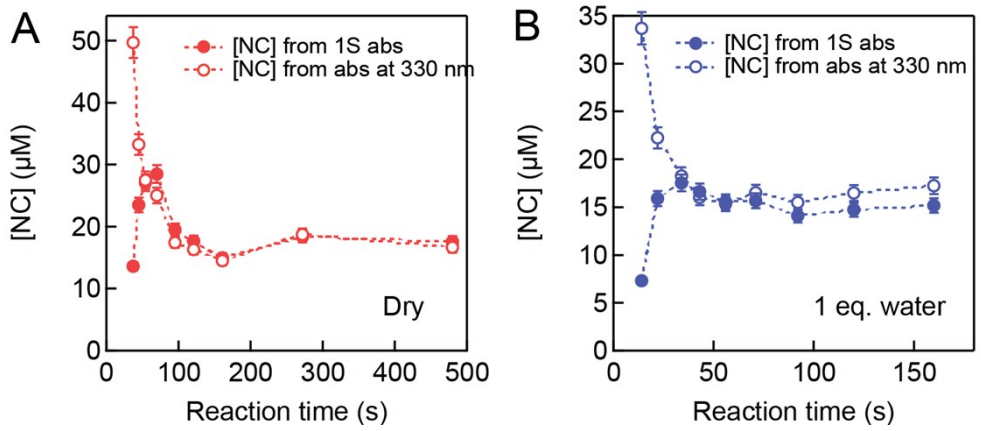

Figure S1. Comparison of nanocrystal concentration calculated using $[NC]_{1S}$ and $[NC]_{3.76eV}$.

The size-dependent extinction coefficients rely on the lowest energy 1S absorbance peak of the regular NCs, which is not convoluted with MSC or CP absorbance. Therefore in the main text we use $[NC]_{1S}$ to obtain the concentration of NCs.

We note that the eventual convergence of the two methods in Figure S1 allows confirmation that MSCs and CPs indeed disappear during the reaction, as discussed in the main text. It is also interesting to note that the increase in $[NC]_{3.76eV}$ compared to $[NC]_{1S}$ at later reaction times with 1 equiv. added water (Figure S1B) is likely due to the the 2nd nucleation event discussed in the main text. This is because the new population of smaller NCs do not influence the larger NC population 1S peak absorbance but do increase the absorbance at 3.76 eV (330 nm).

Multi-peak fitting procedures. We used a multi-peak fitting procedure to extract the width, optical density and position of the 1S absorbance peak (see Figure S1 below). The yield of CdSe in mol, *n*(CdSe), and reaction yield were calculated from [NC] and the volume of a single nanocrystal:

$$n(CdSe) = \frac{[NC]_{S.D.} \cdot V_{NC} \cdot V_{soln} \cdot \rho_{CdSe} \cdot N_A}{M_{CdSe}}$$

$$Reaction\ yield = n(CdSe)/n(CdO)$$

Where ρ_{CdSe} is the density of CdSe (5.816 g/cm^3), M_{CdSe} the molar mass of CdSe (191.4 g/mol), N_A is Avogadro's number, V_{NC} the volume of one NC (cm^3), V_{soln} the volume of the reaction mixture. Reaction yield is based on the amount of limiting reagent, CdO (4.67 mmol).

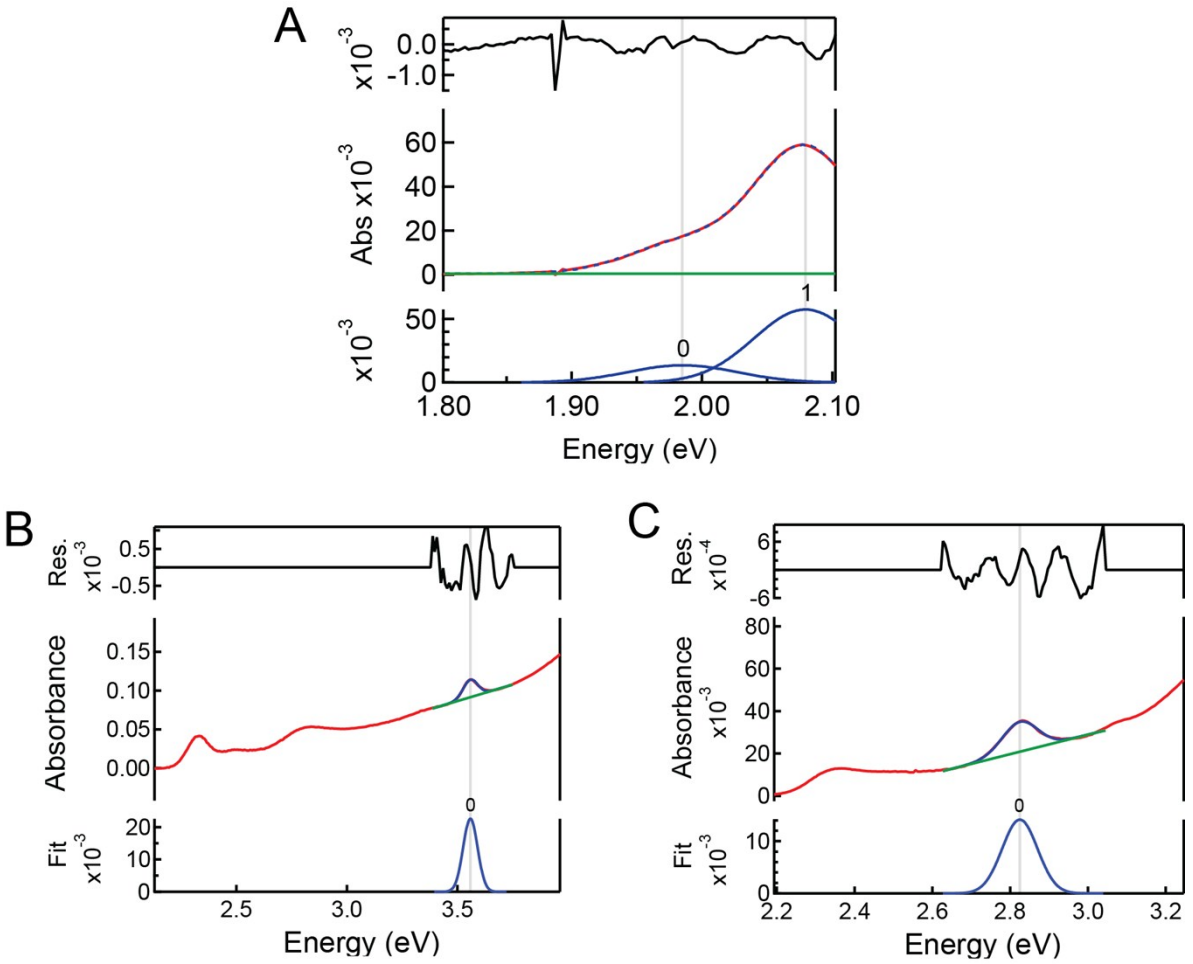

Figure S2. Examples of typical fit results. **(A)** Fitting the first exciton peak absorbance with a low-energy shoulder with two Gaussians. Raw data is in the middle panel as a red line, the constant baseline is green, and the fit is shown as a blue dashed line. The top panel shows the residual (black) and the bottom panel shows the Gaussian fits (blue lines). **(B)** Fit of the MSC-350 to a single Gaussian peak using a linear baseline to approximate the underlying regular NC absorbance. **(C)** Fit of the MSC-437 peak with linear baseline.

Reactions utilising tetradecylphosphonic acid (TDPA) ligand.

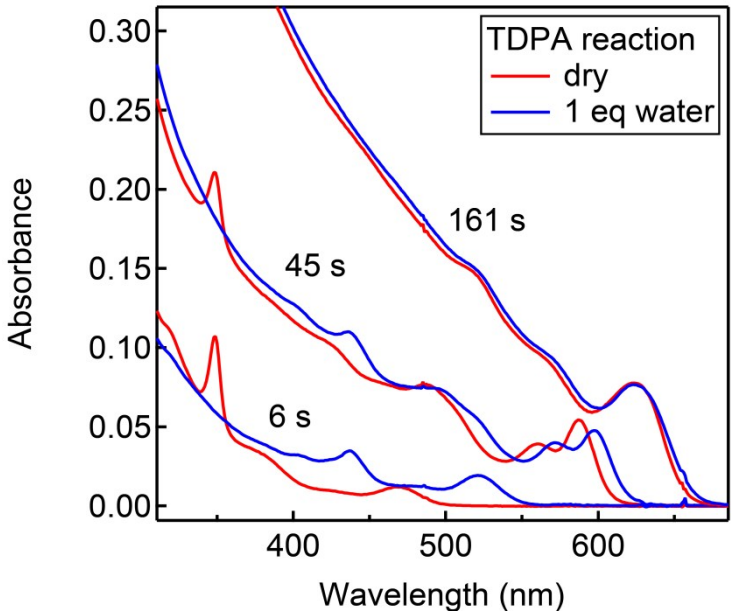

Figure S3. Comparison of selected aliquots taken from dry reaction (red) and reaction with 1 eq. added water (blue) for reactions utilising TDPA ligand instead of ODPA (main text). As with the ODPA ligand, CP-350 is observed in the dry reaction and MSC-437 for the case of added water. The incubation time and growth rate of regular NCs are much faster than for ODPA reactions in the main text.

Reactions with added D_2O compared to H_2O

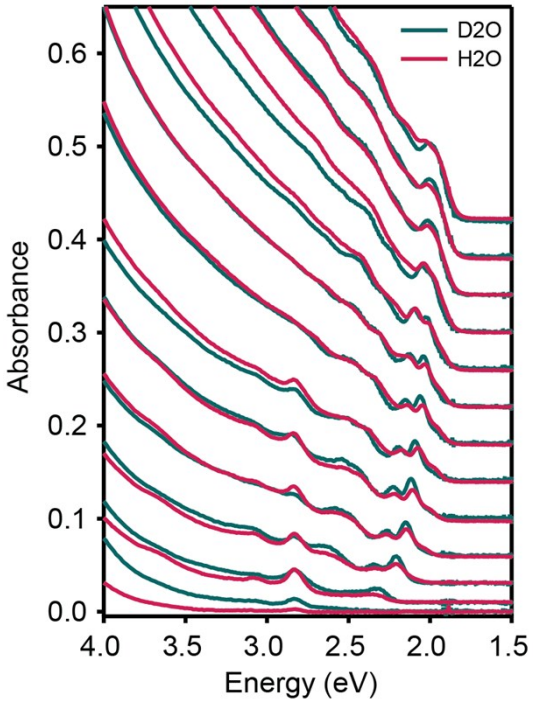

Figure S4. Comparison of reaction aliquot absorbance as a function of reaction time with added water (1 equiv. H_2O, red lines) and added heavy water (1 equiv. D_2O, green lines). Traces are offset vertically with reaction time. Reaction times are, from bottom to top: 5s, 15s, 25s, 35s, 45s, 55s, 70s, 95s, 120s, 160s, 210s, 285s, 480s. No significant difference is observed between reaction aliquots at the same times.

Reactions with reduced concentration of trioctylphosphine (TOP)

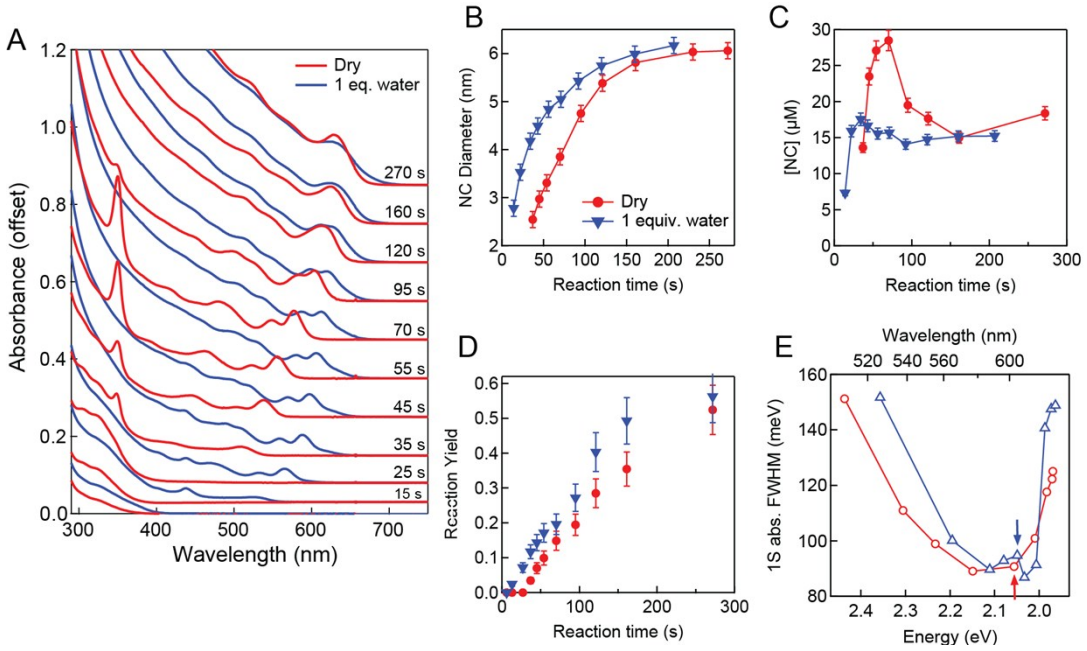

Figure S5. The effect of reduced TOP concentration on CdSe NC reaction dynamics. In these reactions, the addition of TOP prior to TOPSe injection was omitted, giving a final *free* TOP concentration of 0.05 M after TOPSe injection, compared to [TOP] = 0.71 M in Figure 1 of the main text. All other reaction conditions are the same as in Figure 1 of main text. **(A)** Absorbance of reaction aliquots taken throughout reactions (i) without added water (red) and (ii) with 1 eq. added water (blue). Traces are offset vertically with time. First aliquot is at 5 s. CP-350 is observed in the dry reaction and MSC-437 and with added water. **(B)** NC diameter as function of reaction time for (i) dry reaction (red circles) and (ii) with 1 equiv. added water (blue tringles). **(C)** Concentration of CdSe NCs ([NC]) as a function of reaction time. **(D)** Reaction yield (1 = complete conversion of precursor to CdSe) as a function of reaction time. **(E)** FWHM of the 1S absorbance peak plotted against the peak energy for dry and added water reactions. Arrows show where MSC-437 or CP-350 are no longer observed. The data is consistent with the model presented in the main text, where these reaction intermediates disappear at the point where ripening occurs and monomer concentration is lowest.

Discussion of the role of TOP. To further elucidate the role of water we repeated the experiments described in Figure 1 of the main text but skipped the addition of 1.8 mL of TOP after CdO complexation to reproduce the conditions employed previously by Liu *et al.*[2] After the injection of TOPSe the final free TOP concentration in this reaction was 0.05 M, compared to 0.71 M for the reaction used in Figure 1. Analysis of this reaction (absorbance traces, NC diameter, NC concentration and reaction yield as functions of time) is provided in Figure S3. We highlight several key observations from the 0.05 M TOP reaction data in comparison to the reactions with 0.71 M TOP: (i) the incubation periods are noticeably longer with less TOP, but water still decreases the incubation period; (ii) an increased NC growth rate and decreased NC concentration is observed in both cases, and (iii) the reaction with [TOP] = 0.05 M gives a much higher reaction yield with added water than without, in contrast to the similar reaction yields for 0.71 M TOP. These data are consistent with the hypothesis that water increases the precursor consumption rate,[2] and hence increases the reaction yield at any given time. We conclude that TOP masks the effect of water in the data presented in Figure 1, potentially by independently increasing the precursor conversion rate. This effect is independent of the observation of MSC-437 (added water) and CP-350 (dry reaction) intermediates, which is similar to the reactions presented in the main text with higher TOP concentration.

Reaction temperature controls.

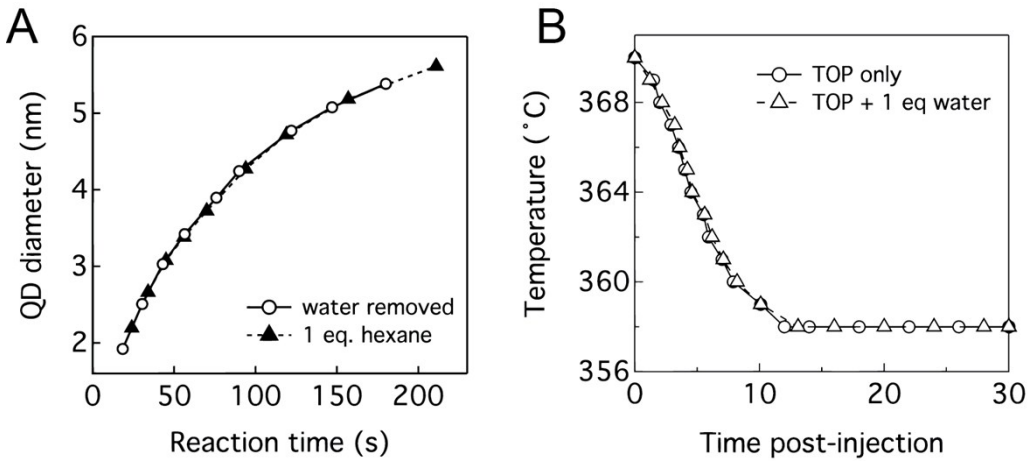

Figure S6. Further control experiments ruling out reaction temperature changes **(A)** Diameter of NCs over time for the same reaction conditions as in Figure 1 of the main text for the dry reaction (open circles) and with 1 equiv. of co-injected hexane (filled triangles). The injection of hexane does not affect reaction. **(B)** Temperature of 3 g TOPO + 1.8 mL TOP (same amounts as reaction in Figure 1 of the main text) after injection of a further 0.5 mL TOP (open circles) and 0.5 mL TOP + 1 equiv. water (filled triangles). The temperature profile is not measurably affected by 1 eq. water.

Extended characterisation & discussion of the structure of CP-350 and MSC-437

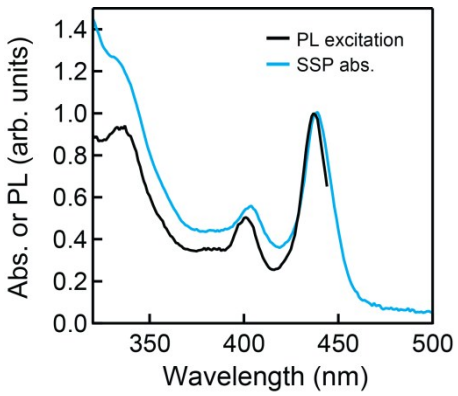

Figure S7. Comparison of absorbance spectrum of MSC-437 cluster isolated by size-selective precipitation (blue trace) and the PL excitation spectrum of the MSC-437 cluster emission from Figure 3C in the main text (black trace).

Discussion of literature regarding CP-350 structure. We have recently shown that the species absorbing at 350 nm in CdSe nanocrystal syntheses is a fibrillar coordination polymer reaction intermediate, CP-350.[3] A persistent peak at 350 nm has been observed before in similar reaction systems incorporating Cd-phosphonate precursors/ligands and TOPO solvent, but was assumed to be a magic-sized cluster rather than a polymer[4-5]. This assumption was based on the work of Soloviev *et al.*[6-7] who reported charged $[Cd_{17}Se_4(SePh)_{24}]^{2+}$ (SePh = selenophenol ligand) clusters with an absorption spectrum featuring a peak at 350 nm. More recently Beecher *et al.*[8] isolated and characterized a neutral tetrahedral $Cd_{35}Se_{20}$ cluster capped with carboxylate and amine ligands with a lowest-energy absorbance band also at 350 nm. However, these clusters are not responsible for the feature at 350 nm in our (and likely other[4-5]) CdSe reactions, because the higher energy absorbance features of the clusters reported by Soloviev and Beecher feature are not present in these reactions.[3]

Discussion of literature regarding MSC-437 structure. There are many reported CdSe MSCs absorbing between 350 nm and 500 nm,[9] but we have found only one instance in the literature of an MSC with the same absorbance as MSC-437, although no attempt was made

to characterize its composition or structure.[10] According to size calibration curves for regular CdSe NCs, which are known to be valid for CdSe MSCs similar to those reported here,[8] MSC-437 would have a diameter of 1.8 nm.[1] However, MSC-437 does not grow and so must be a thermodynamically stable (or metastable) species with a different physical structure and/or ligand shell compared to a regular 1.8 nm NC. Its exact structure remains an open question. In Figure S7 the difference in energy between the first and second exciton peaks and the 1S absorbance peak are plotted for several reactions with added water. Such a plot can be used to determine whether a NC has wurtzite or zinc blende structure, as the energy difference between the two peaks is larger for the zinc blende nanocrystals.[11] In Figure S7, MSC-437 does not fit the trend of regular NCs, which fall onto a line consistent with a single wurtzite crystal structure.[12] This points towards a different crystal structure or an electronic structure that is highly modified by the surface of the cluster.

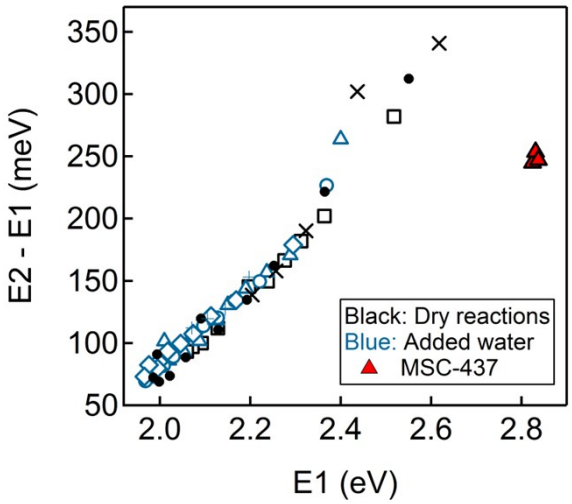

Figure S8. Difference between first absorbance peak energy (E1) and the second absorbance peak energy (E2) as a function of E1 for six different reactions. Each individual reaction is denoted by a different symbol marker; black markers represent dry reactions and blue markers reactions with added water. Data points derived from MSC-437 clusters from reactions with added water are highlighted as red triangles.

Effect of amines on MSC production.

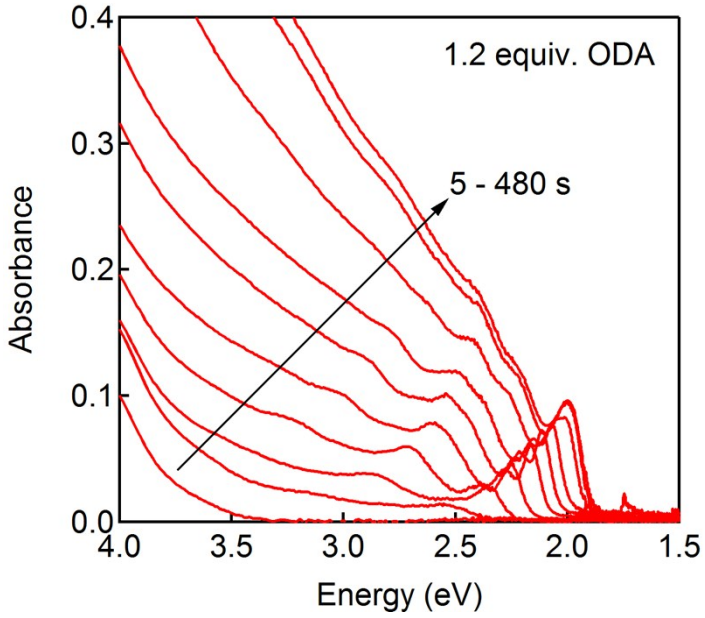

Figure S9. Raw absorbance data of the dry reaction with added octadecylamine (1.2 equiv. vs Cd). No MSCs are observed. All other reaction conditions as described in Methods section of the main text.

Extended data for added alcohol.

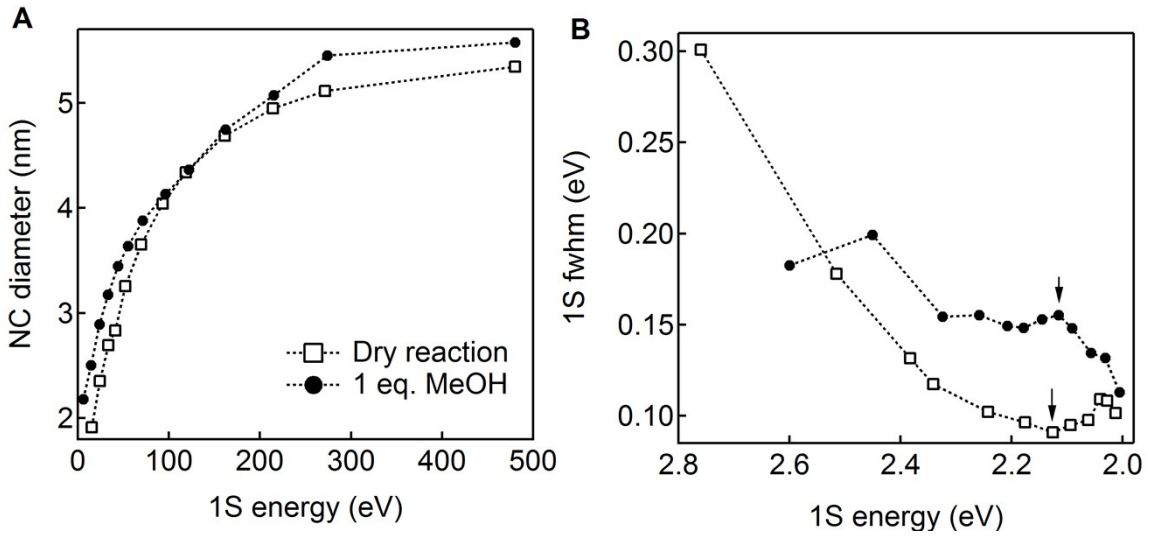

Figure S10. Reproduced data for methanol addition (filled circles) and dry reaction (open squares). Identical reaction conditions were used as described for added methanol reactions in the main text for Figures 5 and 6. **(a)** NC diameter as a function of reaction time. The reaction with added methanol gives a larger initial NC diameter but the growth rate slows (relative to the dry reaction) at around 100 seconds. **(b)** Absorbance 1S peak fwhm plotted against the peak energy. Arrows indicate point when MSCs are no longer observed in the reaction.

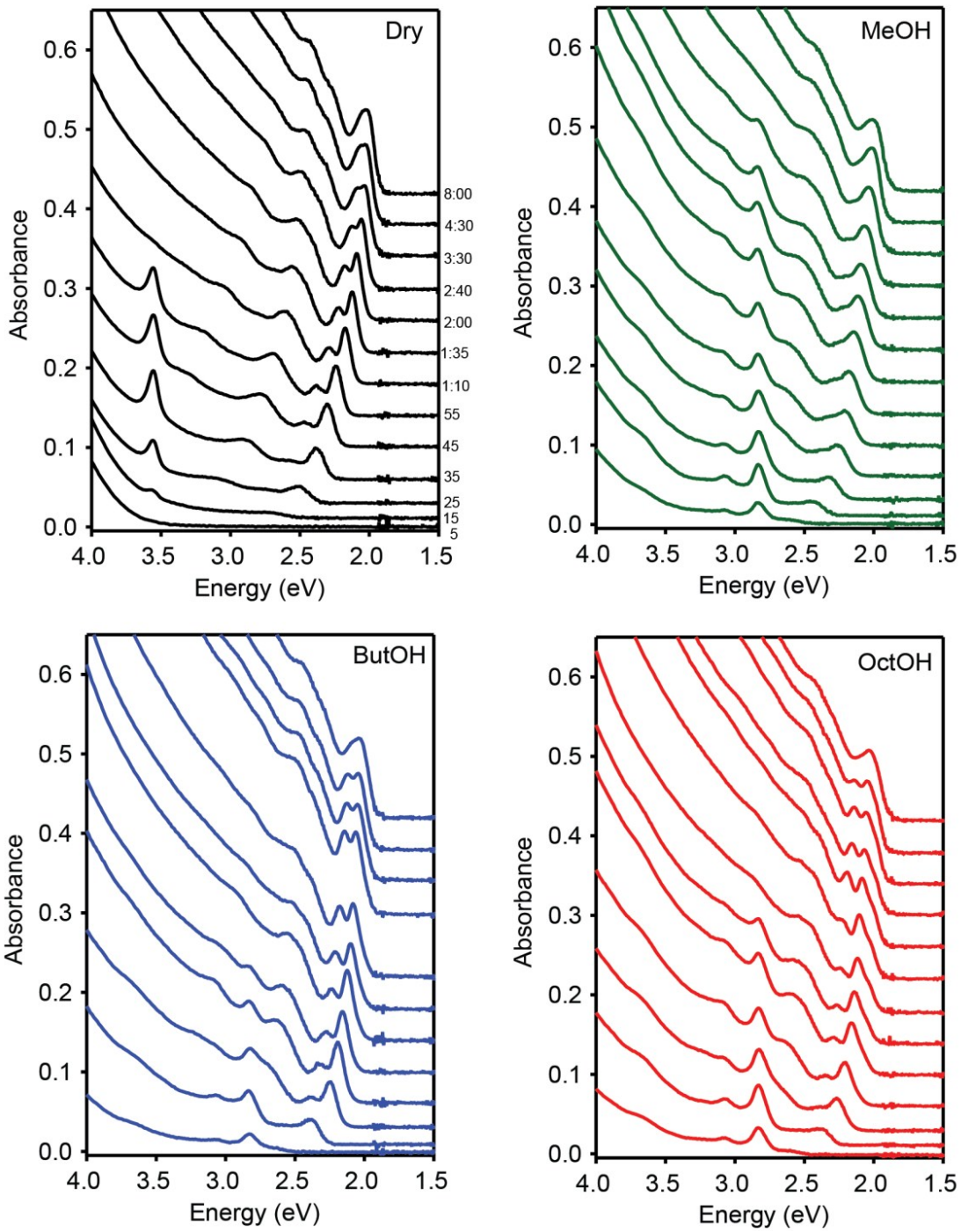

Figure S11. Raw data for added alcohols of different chain lengths. Reaction times in minutes:seconds are shown for the dry reaction and are similar (within ~5 seconds) for other reactions. Distinguishing between C-O or O-H bond scission is difficult, but the similarity between our results for reactions with added methanol, butanol, and octanol favors the mechanism in which there is cleavage of the C-O bond, leaving a surface hydroxyl group.

Second nucleation observation for reactions with added alcohol.

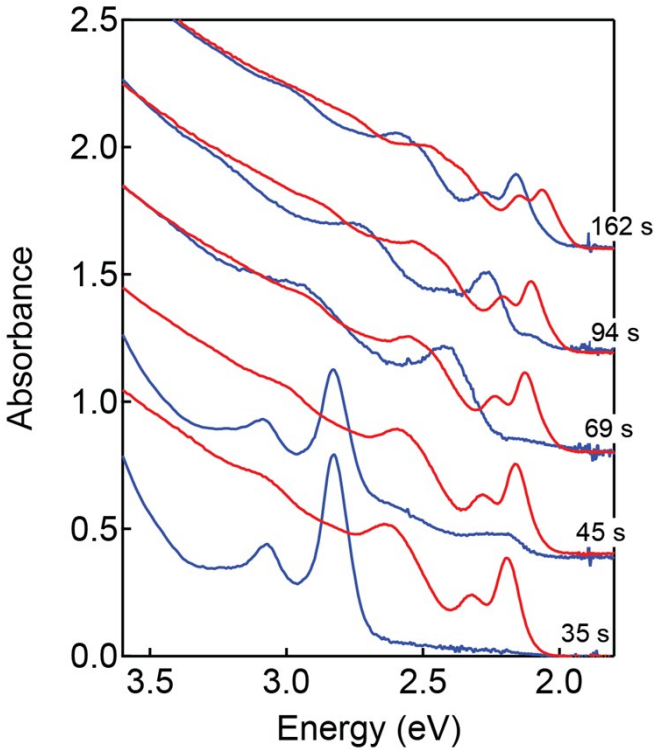

Figure S12. Absorbance of reaction aliquots separated by NC size using SSP, taken during the reaction of Cd-ODPA and TOPSe with 1 equiv. butanol (blue traces in Figure S9). Red lines show the largest NCs obtained via SSP and blue lines show the smallest NCs obtained via SSP. As observed in the main text Figure 6A, at a certain point the MSC species disappears and a new population of small regular NCs is observed, which then grows to eventually merge with the larger regular NC population.

References for Supporting Information

1. Jasieniak, J.; Smith, L.; van Embden, J.; Mulvaney, P.; Califano, M., Re-examination of the Size-Dependent Absorption Properties of CdSe Quantum Dots. *J. Phys. Chem. C* **2009,** *113* (45), 19468–19474.
2. Liu, H.; Owen, J. S.; Alivisatos, A. P., Mechanistic study of precursor evolution in colloidal group II-VI semiconductor nanocrystal synthesis. *J. Am. Chem. Soc.* **2007,** *129* (2), 305-312.
3. Wurmbrand, D.; Fischer, J.; Rosenberg, R.; Boldt, K., Morphogenesis of anisotropic nanoparticles: self-templating via non-classical, fibrillar Cd 2 Se intermediates. *Chem. Commun.* **2018,** *54* (53), 7358-7361.
4. Peng, Z. A.; Peng, X. G., Nearly monodisperse and shape-controlled CdSe nanocrystals via alternative routes: Nucleation and growth. *J. Am. Chem. Soc.* **2002,** *124* (13), 3343-3353.
5. Jiang, Z. J.; Kelley, D. F., Role of magic-sized clusters in the synthesis of CdSe nanorods. *ACS Nano* **2010,** *4* (3), 1561-1572.
6. Soloviev, V. N.; Eichhofer, A.; Fenske, D.; Banin, U., Size-dependent optical spectroscopy of a homologous series of CdSe cluster molecules. *J. Am. Chem. Soc.* **2001,** *123* (10), 2354-2364.
7. Soloviev, V. N.; Eichhöfer, A.; Fenske, D.; Banin, U., Molecular Limit of a Bulk Semiconductor: Size Dependence of the "Band Gap" in CdSe Cluster Molecules. *J. Am. Chem. Soc.* **2000,** *122* (11), 2673-2674.
8. Beecher, A. N.; Yang, X.; Palmer, J. H.; LaGrassa, A. L.; Juhas, P.; Billinge, S. J.; Owen, J. S., Atomic structures and gram scale synthesis of three tetrahedral quantum dots. *J. Am. Chem. Soc.* **2014,** *136* (30), 10645-10653.
9. Yu, K.; Hu, M. Z.; Waing, R. B.; Le Piolet, M.; Frotey, M.; Zaman, M. B.; Wu, X. H.; Leek, D. M.; Tao, Y.; Wilkinson, D.; Li, C. S., Thermodynamic Equilibrium-Driven Formation of Single-Sized Nanocrystals: Reaction Media Tuning CdSe Magic-Sized versus Regular Quantum Dots. *J. Am. Chem. Soc.* **2010,** *114* (8), 3329-3339.
10. Yu, K., CdSe Magic-Sized Nuclei, Magic-Sized Nanoclusters and Regular Nanocrystals: Monomer Effects on Nucleation and Growth. *Adv. Mater.* **2012,** *24* (8), 1123-1132.
11. Mohamed, M. B.; Tonti, D.; Al-Salman, A.; Chemseddine, A.; Chergui, M., Synthesis of high quality zinc blende CdSe nanocrystals. *J. Phys. Chem. B* **2005,** *109* (21), 10533-10537.
12. Washington, A. L.; Foley, M. E.; Cheong, S.; Quffa, L.; Breshike, C. J.; Watt, J.; Tilley, R. D.; Strouse, G. F., Ostwald's Rule of Stages and Its Role in CdSe Quantum Dot Crystallization. *J. Am. Chem. Soc.* **2012,** *134* (41), 17046-17052.